Visualizing the Electrical Structure of Power Systems

P. Cuffe, *Member, IEEE*, and A. Keane, *Senior Member, IEEE*

***Abstract*— Recent work, using electrical distance metrics and concepts from graph theory, has revealed important results about the electrical connectivity of empiric power systems. Such structural features are not widely understood or portrayed. Power systems are often depicted using unenlightening single line diagrams, and the results of load flow calculations are often presented without insightful elucidation, lacking the necessary context for usable intuitions to be formed. For system operators, educators, and researchers alike, a more intuitive, accessible understanding of a power system's inner electrical structure is called for. Data visualization techniques offer several paths towards realizing such an ideal. The present paper proposes various ways electrical distance might be defined for empiric power systems, and records how well each candidate distance measure may be embedded in two dimensions. The resulting two-dimensional projections form the basis for new visualizations of empiric power systems, and offer novel, useful insights into their electrical connectivity and structure.**

***Index Terms*—Data visualization, power system structure, Z_{bus} matrix**

I. Introduction

As early as 1993, the authors of [1] emphasised the value of visualizing power system data using a "*natural encoding that most people could grasp easily and without interpretation*". This injunction echoes Edward Tufte's seminal works on effective data visualization [2-4]. By 2012, the partial review of [5] noted that there still no "*best practice*" for visually representing power system data. Since the mid 1990s, various researchers have proposed ways of improving the humble single line diagram, with Dr. Thomas Overbye and his collaborators making noteworthy contributions here ([6] surveys several of his contributions). Some typical examples from the literature: [7, 8] added coloured contour lines to portray voltage magnitudes; [9, 10] added a third-dimension above the diagram plane to visualize various data; [11] discussed ways of superimposing real-time market data. The authors of [5] noted the recent paucity of works building on these contributions: "*since then, surprisingly few new ideas […] have been presented*"

One shortcoming in each of the foregoing works is that plotted bus positions remain substantially arbitrary, and exhibit no meaningful "*natural encoding*". While there are some examples in the literature of algorithmic bus positioning [12-14], none of these methods locate nodes in a way that is defensibly electrically meaningful. A rare example of system diagrams based on meaningful electrical distances is given in [15], though results are only shown for a small 14 bus system.

For cognitive reasons, two nodes drawn in close proximity are likely to be perceived as being in the same group or cluster [16, 17]. As such, an arbitrarily laid out single line diagram may give the erroneous impression that an isolated node is well-connected, or that a central node is electrically remote.

A first step to rectify this would be to scale each branch's length such that it corresponds to its impedance. Force-directed graph layout algorithms (e.g [18]) can achieve this, and they have been deployed in this role [12, 19]. The treatment of [12] is comprehensive, and the visualization they present was shown in usability trials to aid system operators in identifying salient features of the power system, for instance allowing rapid and easy recognition of several diverse synchronous islands. The authors concluded: "*there is a tremendous value to leveraging the existing visualization knowledge base to a field that has traditionally not expended significant resources in the area*"

This paper takes its cue from this exhortation, and also seeks to extend, and articulate, some recent results on electrical connectivity and centrality in empiric power systems. Electrical power systems can be viewed as undirected complex graphs; from this perspective [20], which disregards the physics of electrical power flow, various works [21-25] have sought to classify empiric power systems using such classic topological descriptors as node degree. While consensus has not always been reached, the state of the art allows the synthesis of artificial networks that resemble existing power systems in their topological structure [26].

One motivation for taking a graph theory approach to power systems is to better understand system vulnerability to attack or component failure (as in [24, 27-29]), especially given the interesting observed fact that the severity of power system black-outs [30], like terrorist atrocities [31], follow a power-law distribution. This is plausibly a consequence of some structural power-law distribution in electrical networks, however trying to infer the vulnerability of a power system from basic topological measures remains quite dubious [32]. Purely topologic models of a power system offer only limited insight into how a system will behave, as they neglect the physical flow equations that govern power propagation through the network.

More useful insights are possible when the electrical realities of a power grid are united with a complex graphs analytic perspective. For instance, [33] defined a meaningful measure of electrical distance on power systems, and used it to show that empiric systems tend to have a number of core nodes possessing high "*electrical centrality*". This fact is not properly revealed by purely topologic centrality metrics, nor is

This work was conducted in the Electricity Research Centre, University College Dublin, Ireland, which is supported by the Commission for Energy Regulation, Bord Gáis Energy, Bord na Móna Energy, Cylon Controls, EirGrid, Electric Ireland, EPRI, ESB International, ESB Networks, Gaelectric, Intel, SSE Renewables, UTRC and Viridian Power & Energy.

P. Cuffe is supported by the European Community's Seventh Framework Programme (FP7/2007-2013) under grant agreement n° 608732A

this perspective emphasised in traditional electrical engineering approaches. Drawing on similar insights, [34] used cognate concepts of electrical proximity to divide a power system into meaningful network zones; [35] used spectral clustering and embedding techniques to partition and visualise power systems; [36] defined an electrically meaningful centrality metric to identify critical components; [37] used an impedance-based graph metric to assess a power system's robustness to cascading failure.

The novel techniques given in the present work permit a deeper understanding of the power grid's role as an interconnected electromechanical system of systems. The principal methodology used is multidimensional scaling, which allows electrical distance measures to be projected into a visually tractable two-dimensional plane. For the first time, this work defines a number of candidate electrical distance measures, and records how well each can be projected into two dimensions. To this end, a valuable technique for calculating inter-node Thevenin impedances is discussed. The application of multidimensional scaling with certain distance measures reveals an entirely new perspective on power systems, where the electrical realities of the network are explicitly portrayed. This new portrayal offers new insights on the electrical structure, and voltage performance, of power systems, and also shows the distinct qualities of the transmission and distribution systems. Finally, a validatory application is presented, where a power system is divided into electrical zones based on its two-dimensional projection.

The visualization methodology is described in Section II. Results, and example layouts, for various common test power systems are provided in Section III. A partitioning application, and partial validation, of the technique is given in Section IV, with discussions and conclusions given in V.

II. Visualization Methodology

A. Multidimensional Scaling

How can a matrix of inter-node electrical distances, howsoever defined, be converted to a meaningful representation of the power system? The well-established statistical technique of multidimensional scaling [38, 39] offers the required visualization capability [15, 40].

Multidimensional scaling methods use iterative techniques to position each node, in an arbitrary number of dimensions, N, so that the fitted distances between node pairs, d_{ij}, are maximally consistent with the desired input distances, d^*_{ij}.

The present work uses the Sammon stress function [41], which defines the error function, E, to be minimised thusly:

$$E = \frac{1}{\sum_{i<j} d^*_{ij}} \sum_{i<j}^{N} \frac{(d^*_{ij} - d_{ij})^2}{d^*_{ij}} \tag{1}$$

This function can be minimized using iterative gradient descent methods, and its final value suggests a goodness-of-fit for the embedding of d^*_{ij} into the N chosen dimensions. Multidimensional scaling is one of many dimensionality-reduction techniques [42]. It is selected in this instance because it explicitly seeks to preserve inter-node distances, and so the resulting projections can be dimensioned in explicitly electrical units.

B. Candidate Distance Measures

The recent work of Hines et al. [22, 33, 43] as well as Bompard et al. [27, 44, 45] points towards the role of inter-node electrical distance measures in elucidating the structural features of power systems. Earlier works have used electric distance measures in a number of roles: [46] introduced node-to-node voltage attenuation distances and used them in identifying voltage control zones; [47] used the same in assessing system voltage security; [48] to partition a system into localized reactive power markets; [49] used impedance sub-matrices to relate load and generator voltages as a distance metric for transmission use-of-system charging; later, and seemingly independently, Abdelkader et al. [50-52] used closely related sub-matrices for power flow tracing and loss allocation purposes.

A number of potential electrical distance measures of differing complexity are considered in the present work, relying variously on the simple topology of the system, the electrical connectivity of the system, and the Jacobian matrices formed in solving the ac power flow problem.

These various measures are being trialled, in the first instance, to ascertain which can meaningfully be projected onto a two-dimensional plane. The motivation for such a projection is twofold: firstly, visualization is an established exploratory practice for revealing structures of interest in complex networks [53], and secondly, to demonstrate novel ways of representing power systems such that their operation can be understood in a more intuitive way, per [1]. Additionally, the range of distance measures considered allows instructive comparisons to be made between them.

1) Thevenin Impedance Distance

Consider first an intuitive measure, where the distance between two nodes is the equivalent Thevenin impedance between them, being the parallel combination of all impedance paths connecting them. Usefully, this can be calculated directly from the system's Z_{bus} matrix, which is simply the matrix inverse of the system's Y_{bus} matrix, the fundamental topological descriptor of the electrical system's connectivity, corresponding [35] to the Laplacian matrix [54] for generic networks. The relevant calculation is given by Klein in [55] as:

$$Z^{thev}_{ij} = Z_{ii} + Z_{jj} - Z_{ij} - Z_{ji} \tag{2}$$

where Z_{ij} denotes the (complex-valued) element in the i^{th} row and j^{th} column of the Z_{bus} matrix, being the mutual impedance between those two buses. The symmetry of the Z_{bus} matrix, in the absence of active elements [56], implies that $Z_{ij} = Z_{ji}$. Note that we can also decompose this into resistance and reactance, with $R^{thev} = Re(Z^{thev})$ and $X^{thev} = Im(Z^{thev})$

This manipulation gives the *Klein Resistance Distance* between the two nodes, in the power systems context equivalent to the Thevenin impedance [57]. This graph

distance measure is quite popular across various fields that model systems by analogy with electrical circuits (e.g communication networks in [58], fullerene isomers in [59], and genetic structuring across heterogeneous landscapes in [60]). It is perhaps surprising that it is not commonly used in the electrical ambit where it seems most directly applicable, though some rare examples in the power systems area exist [45, 61].

In transmission systems, branches are assumed to have a high *X/R* ratio, permitting application of the dc power flow approximations [62, 63]. Under these assumptions, the $|Z^{thev}_{ij}|$ distance predicts the change in voltage angle required to transmit a unit of active power from one bus, *i*, for reception at *j*, holding all other system quantities constant.

Work such as [64] has proposed system voltage angle separations as being a key metric of system robustness, while [65] concludes that "*phase angle differences serve as an excellent measure of system stress*". Conceptually, large voltage angle differences arise when substantial power flows are transacted over long electrical distances: the $|Z^{thev}|$ distance may help to visualize power systems so that such transactions can be easily identified.

Note that the $|Z^{thev}|$ distance is independent of system loading, and can be calculated without power flow techniques. Crucially, it properly accounts for all the available current paths between two nodes; compare work such as [66, 67] where the impedance between nodes is approximated by summing impedances along the topologically shortest path.

The sum of all inter-node resistance distances is generally defined as the *Kirchoff Index* of a graph [55], a graph measure believed to be closely related to network robustness [68]. Recent work [37] has found a close relationship between this measure and a power system's vulnerability to cascading failures.

Finally, note that resistance distances are closely related to random walks on graphs [69], and to the eigenvalues and eigenvectors of the graph's Laplacian, and they can be calculated by such means [70-72]. This is an example of spectral graph theory [54], whose application to power system problems has only recently emerged [35, 61, 73-76].

2) Mutual Impedance Distance

Certain authors [43] have simply used the off-diagonal elements of a system's Z_{bus} matrix to populate a system distance matrix. The diagonal elements of the Z_{bus} matrix are not generally zero, suggesting that it does not inherently encode distance information. The mutual impedances can be interpreted as giving the voltage at the *i* bus for a unit current injection at *j*, assuming open circuit conditions at all other buses:

$$Z_{ij} = V_i \Big/ I_j \Big| I_{n \neq j} = 0 \tag{3}$$

For the present work, the requirement for zeroes on the main diagonal is artificially enforced as follows, to populate the Z^{mut} distance matrix as follows:

$$Z^{mut}_{ij} = \begin{cases} Z_{ij} \,|_{i \neq j} \\ 0 \,|_{i=j} \end{cases} \tag{4}$$

3) Power Transfer Distance

The dc power flow approximations can be further extended to capture the aggregate effect on branch flows for a power transfer between a sending bus *i* and a receiving bus *j*. While $|Z^{thev}_{ij}|$ indicates the voltage angle change needed to realise this, how will this voltage angle shift affect flows in each branch of the system? Such altered branch flows have been described in the regulatory context using *Power Transfer Distribution Factors* [77]. Using a similar approach, a new electrical distance measure is here proposed, PT_{ij}. This gives the total shift in active power flows, F^P, across all branches, *B*, in the entire system, for a unit active power injection at *i* and withdrawal at *j*:

$$PT_{ij} = \sum_B \left| F^P_B \right|_{P_i=1, P_j=-1} \tag{5}$$

Note that this measure takes an absolute value for power flow shifts: for a particular transaction, flows on certain branches will increase, and on others will decrease, while it is the aggregate shift that is being captured. The *PT* distance is closely related to the ideas of net-ability and power transfer capacity as described in [44], and also recalls current flow centrality metrics defined for generic graphs [78].

The PT_{ij} distance is proposed to indicate how much of a network's assets are used in facilitating a transaction between two nodes. Given the fact that branches in a power system have maximum current limits, it seems plausible that regions separated by high PT_{ij} values will not be able to trade much power, and may exhibit divergent locational marginal prices [79].

4) Jacobian Distances

The solution of the load flow problem yields a useful matrix of power flow sensitivities, the *Jacobian*:

$$\begin{bmatrix} \Delta P \\ \Delta Q \end{bmatrix} = J \begin{bmatrix} \Delta \theta \\ \Delta V \end{bmatrix} \tag{6}$$

This matrix relates the effect of an incremental complex power injection at a bus, *i*, on voltage magnitudes and angles at other buses, *j*. The authors of [33, 34] point out that the inverse of this matrix can also be manipulated to find Klein resistance distances [55]. Four matrices can be extracted from the Jacobian:

$$J = \begin{bmatrix} J_{P\theta} & J_{PV} \\ J_{Q\theta} & J_{QV} \end{bmatrix} = \begin{bmatrix} \partial P / \partial \theta & \partial P / \partial V \\ \partial Q / \partial \theta & \partial Q / \partial V \end{bmatrix} \tag{7}$$

The first two correspond to dc power flow intuition: $J_{P\Theta}$, which relates nodal active power injections, *P*, to voltage angle changes, Θ; and $J_{QV,}$ which relates reactive power injections, *Q*, to voltage magnitude changes, *V*. We can also

extract the contrary matrices, J_{PV} and $J_{Q\Theta}$, whose interpretation confounds the expectations of dc power flow. By taking the matrix pseudo-inverse [80] of each of these, notated J^{-1}, we can apply the Klein distance formula to attain power flow sensitivity matrices that are conveniently free of slack-bus dependence:

$$\Delta\theta_{ij}/\Delta P_{ij} = (J_{P\theta}^{-1})_{ii} + (J_{P\theta}^{-1})_{ij} - (J_{P\theta}^{-1})_{ji} - (J_{P\theta}^{-1})_{jj} \quad (8)$$

$$\Delta V_{ij}/\Delta Q_{ij} = (J_{QV}^{-1})_{ii} + (J_{QV}^{-1})_{ij} - (J_{QV}^{-1})_{ji} - (J_{QV}^{-1})_{jj} \quad (9)$$

$$\Delta V_{ij}/\Delta P_{ij} = (J_{PV}^{-1})_{ii} + (J_{PV}^{-1})_{ij} - (J_{PV}^{-1})_{ji} - (J_{PV}^{-1})_{jj} \quad (10)$$

$$\Delta\theta_{ij}/\Delta Q_{ij} = (J_{Q\theta}^{-1})_{ii} + (J_{Q\theta}^{-1})_{ij} - (J_{Q\theta}^{-1})_{ji} - (J_{Q\theta}^{-1})_{jj} \quad (11)$$

To clarify the notation: the first of these measures describes the incremental change in voltage angle difference between two nodes, ($\Delta\Theta_i$ - $\Delta\Theta_j$), for an incremental injection of active power at *i*, and withdrawal at *j*, holding all other quantities constant.

5) Topological Geodesic Distance

This is a fundamental topological distance measure, recording the minimum number of branches that must be traversed to travel from node *i* to node *j*. This disregards the electrical realities of a power system, treating it instead as a simple unweighted, undirected graph. It can be calculated by a number of algorithms, all somewhat computationally intensive, the most popular of which is given by Djikstra [81].

The geodesic distance, $d^{geo}{}_{ij}$, provides a lower bound to the PT_{ij} measure: where the connection between *i* and *j* is purely radial, as is typical in distribution systems [82], the two measures will be equal.

III. Results

TABLE I
ACHIEVED SAMMON STRESS VALUES, *E*, FOR EACH TEST SYSTEM ($N = 2$)

		***rts_1_area* [83]**	***case30* [84]**	***case39* [85]**	***rts_2_area* [83]**	***case57* [86]**	***case118* [86]**	***case300* [86]**
Thevenin Impedance	$\lvert Z^{thev}\rvert$	0.0261	0.0328	0.045	0.0229	0.0256	0.0333	0.0316
Jacobian	$\Delta\theta/\Delta P$	0.0317	0.0319	0.0377	0.0306	0.0294	0.0409	0.0195
Shortest Path	d^{geo}	0.0267	0.0457	0.0153	0.0165	0.059	0.0281	0.0349
Power Transfer	PT	0.0275	0.0447	0.0203	0.0295	0.0485	0.0383	0.0453
Jacobian	$\Delta V/\Delta Q$	0.0446	0.0769	0.0437	0.0293	0.0284	0.0289	0.0187
Jacobian	$\Delta V/\Delta P$	0.0243	0.1462	0.0417	0.1847	0.0298	0.1073	0.1769
Mutual Impedance	$\lvert Z^{mut}\rvert$	0.1267	0.1453	0.1266	0.0914	0.1457	0.0397	0.3624
Jacobian	$\Delta\theta/\Delta Q$	0.1939	0.1329	0.2558	0.3363	0.1489	0.291	0.0728

TABLE II
LINEAR COEFFICIENTS OF DETERMINATION BETWEEN SELECTED DISTANCE MEASURES

	rts_1_area	***case30***	***case39***	***rts_2_area***	***case57***	***case118***	***case300***
R^2 ($\lvert Z^{thev}\rvert$, $\Delta\theta/\Delta P$)	0.9929	0.9972	0.9836	0.9827	0.9962	0.954	0.9951
R^2 ($\lvert Z^{thev}\rvert$, $\Delta V/\Delta Q$)	0.7667	0.9302	0.9724	0.9396	0.9933	0.9804	0.9927
R^2 (PT, d^{geo})	0.8396	0.8398	0.9253	0.8604	0.8609	0.9057	0.8988
R^2 (X^{thev}, R^{thev})	0.9077	0.7927	0.6635	0.9275	0.7821	0.9579	0.6937
R^2 ($\lvert Z^{thev}\rvert$, PT)	0.4086	0.4821	0.6457	0.697	0.464	0.8109	0.0099

A. Implementation

Multidimensional scaling and related visualizations were performed in MATLAB [87], and power system calculations were performed using the MATPOWER package [88]. Seven different test power systems, ranging in size from 24 to 300 buses, were considered.

B. Distance Measure Suitability

Interpreting the goodness-of-fit for a multidimensional scaling solution requires care [89]; while simulation studies on random distance data offer some insight on what stress values to anticipate [90, 91], as does Kruskal's [38] original rule-of-thumb for his stress function[2]; these alone do not fully capture the quality of a mapping. The Sammon stress values in Table I should be interpreted in this light, bearing in mind, too, that as they are the result of a randomly-initiated iterative process, they are subject to some variation. They are sorted in

[2] He suggested these thresholds: .20 = poor, .10 = fair, .05 = good, .025 = excellent, and .00 = perfect.

ascending order, to identify which distance measures tend to have the most meaningful embedding in two dimensions (N = 2).

Fortunately, several of the candidate measures seem to embed consistently well into two dimensions. The $|Z^{thev}|$ measure is the best performing, showing that the impedance structure of a power system has a fundamentally two-dimensional interpretation. It is useful and encouraging that this impedance structure can be portrayed in two dimensions with minimal distortion.

Considering all the candidate measures, they appear to sort themselves into two groups: the upper five seem quite satisfactory, whereas the bottom three do not. Notably, these latter three measures do not command a meaningful intuitive interpretation. One does not expect the $\Delta\Theta/\Delta Q$ Jacobian measure to be insightful, as voltage angle separations are not a driver of reactive power flows; likewise, the $\Delta V/\Delta P$ metric is at odds with conventional expectations for active power flows on a transmission system. Finally, the $|Z^{mut}|$ metric does not perform well as a distance measure, a result anticipated by its non-zero diagonal components.

C. Linear Regressions Between Distance Measures

From Table II, it is seen that the $\Delta\Theta/\Delta P$ and $\Delta V/\Delta Q$ measures are closely linearly related to $|Z^{thev}|$, and this explains the similar stress values achieved for these measures in Table I. These Jacobian sensitivities necessarily derive from the underlying impedance structure of the power system, which is now seen to possess a substantially two-dimensional character.

From Table II one can also note a reasonably close relationship between PT and d^{geo}, which shows, surprisingly, that even a naïve topological distance function can approximate how power flows in an electrical network. Interestingly, regressing PT against the electrically meaningful $|Z^{thev}|$ does not reveal pronounced linear correlation. Indeed, this comparison is quite heterogeneous across the six power systems, with the 300 bus system showing practically no linear correlation between $|Z^{thev}|$ and PT. Finally, note that in terms of inter-node Thevenin equivalent distance, X/R ratios are not generally consistent, as revealed by the lack of substantive linear correlation between R^{thev} and X^{thev}.

From the foregoing discussion, it is clear that our five well-performing distance measures duplicate each other to a substantial degree. For the remainder of this paper, $|Z^{thev}|$ will be used to describe the electrical connectivity between buses, given its direct calculation and intuitive interpretation, and PT will be used to capture the flow-sensitive connectivity between buses.

D. Example Layouts

Space constraints preclude the display of all layouts represented in Table I, so only the more illuminating examples are provided here. Colour and line thickness are both used to indicate bus and branch operating voltage: a legend is shown in Fig. 1. As these diagrams are intricate they are best viewed in colour, as available in the electronic version of this paper.

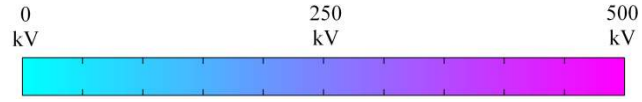

Fig. 1 Nominal voltage colour scale

1) IEEE 30 Bus System

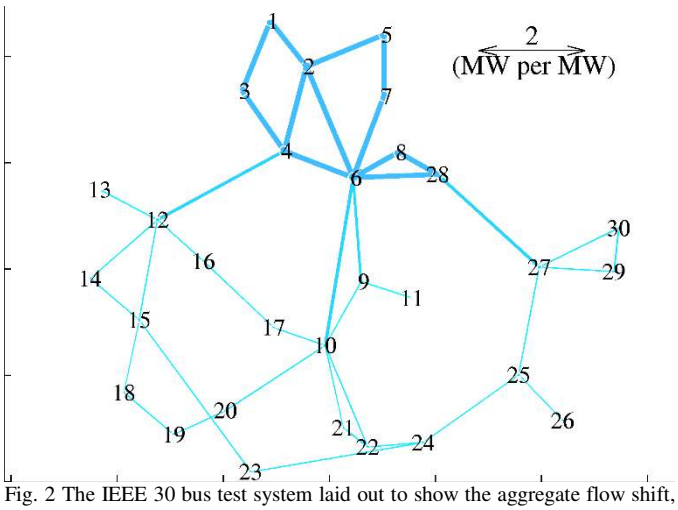

Fig. 2 The IEEE 30 bus test system laid out to show the aggregate flow shift, PT, for each node-to-node transaction

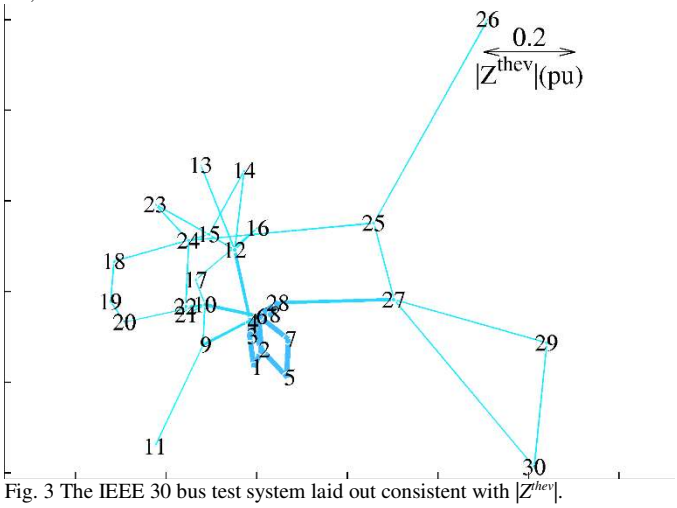

Fig. 3 The IEEE 30 bus test system laid out consistent with $|Z^{thev}|$.

The diagram in Fig. 2 presents a new perspective on the IEEE 30 bus system. One feature this diagram brings to light is the comparative ease with which power can be transacted across the transmission (132 kV) network. These nodes form a small core in the diagram, indicating that power transactions between them are relatively efficient in their use of system assets. Around this core are the 33 kV distribution buses.

The $|Z^{thev}|$ impedance layout of this system, in Fig. 3, shows an even more pronounced clustering of the higher voltage buses. They sit within a core with a diameter of ~ 0.1 pu. As such, power can be transacted around this core with only minor voltage angle separations. The 33 kV system is here far greater in extent, with certain buses (e.g 26, 29 and 30) clearly quite electrically remote from the central core. It is not coincidental that 30 was identified by [92] as being a particularly voltage-weak bus.

The length of the transformer branches is notable, clearly showing how the non-negligible reactance of transformers creates a substantial electrical separation between the various

voltage levels in a power system. (These transformer connect to lower-voltage buses 27, 12, 10 and 9)

Both Fig. 2 and Fig. 3 show that the 30 bus system is somewhat unrepresentative of real power systems. We would expect the 33 kV distribution buses to fully encircle the central core, whereas here they only connect at three distinct buses, emphasising that the distribution circuits at other transmission nodes have not been included in this test system specification.

2) IEEE RTS96 Test System

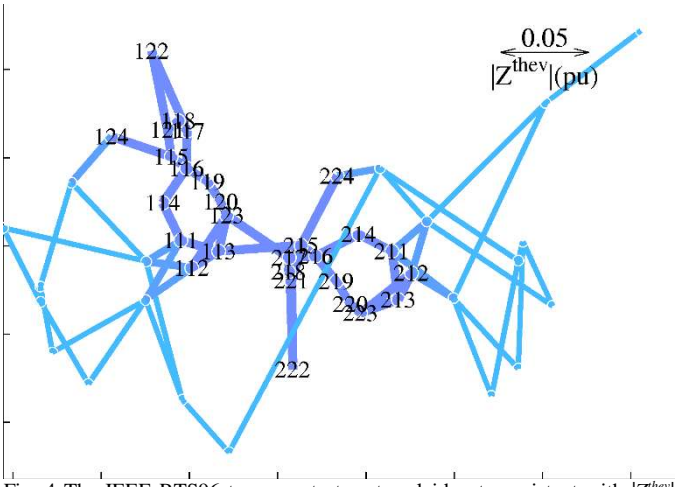

Fig. 4 The IEEE RTS96 two area test system laid out consistent with $|Z^{thev}|$

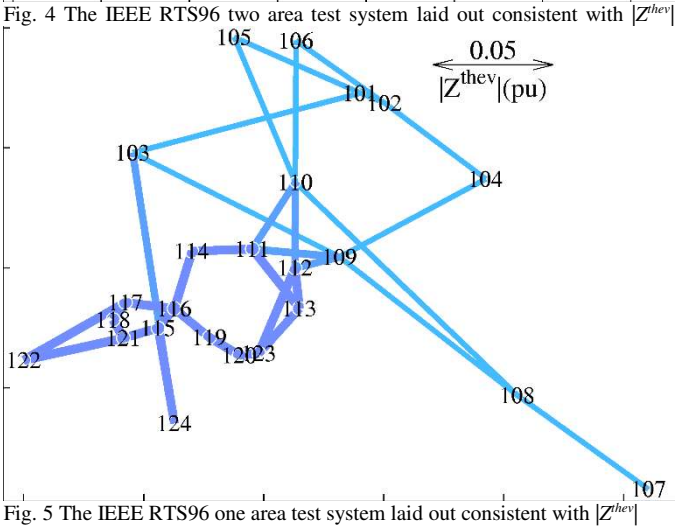

Fig. 5 The IEEE RTS96 one area test system laid out consistent with $|Z^{thev}|$

The impedance structure of the RTS96 test system, in both its one and two area incarnations, is shown in Fig. 4 and Fig. 5. The representation of Fig. 4 recalls the structure of the 30 bus system (Fig. 3) with the higher voltage (230 kV) buses forming an electrically cohesive core of the system. As before, the lower-voltage buses are not homogeneous in their peripherality, with two buses (207 and 208) notably electrically remote, at the top right of the figure. The system is also largely symmetric from left-to-right: this is because the two area system specification simply connects together two copies of the one area system [83], which is shown in Fig. 5.

Previous loadflow simulation work by the authors [93] has examined regional reactive power requirements and voltage performance on the RTS96 single-area system. Two buses, 107 and 108, showed consistently unacceptable voltage performance that could be only be remedied by constraining-on generation at bus 107. The visualization of Fig. 5 makes it very clear that these buses are electrically remote, making obvious the difficulties of transmitting reactive power to support voltages there. By contrast, the canonical system representation of Fig. 6 obscures the dysfunctional lack of connectivity for these buses. Indeed, the unusually exhaustive system description in [83], building on [94, 95], nowhere notes or anticipates voltage problems for these buses.

The lesson is clear: meaningful system representations show important electrical features that would otherwise be passed over, even by sophisticated professionals such as those who authored [83]. Without portraying the two-dimensional impedance structure of a power system, its voltage performance can only be gauged with cumbersome methods, such as the loadflow studies in [93]. The novel visualization promotes insight and understanding; the traditional diagram impedes these.

Finally, it is interesting to note that the difference in scale between Fig. 4 and Fig. 5 is only slight. Even though the two-area system is effectively a two-fold duplication of the one-area, it is erroneous to imagine that its extent doubles in electrical terms. For the one-area system, the maximum $|Z^{thev}|$ impedance between any two nodes is 0.2616 pu; for the two area it is 0.3533 pu, a growth of 35.1%. In *PT* terms, the one area has a maximum separation of 8.43 MW/MW; the two area, 13.84 MW/MW, a growth of 64.2%.

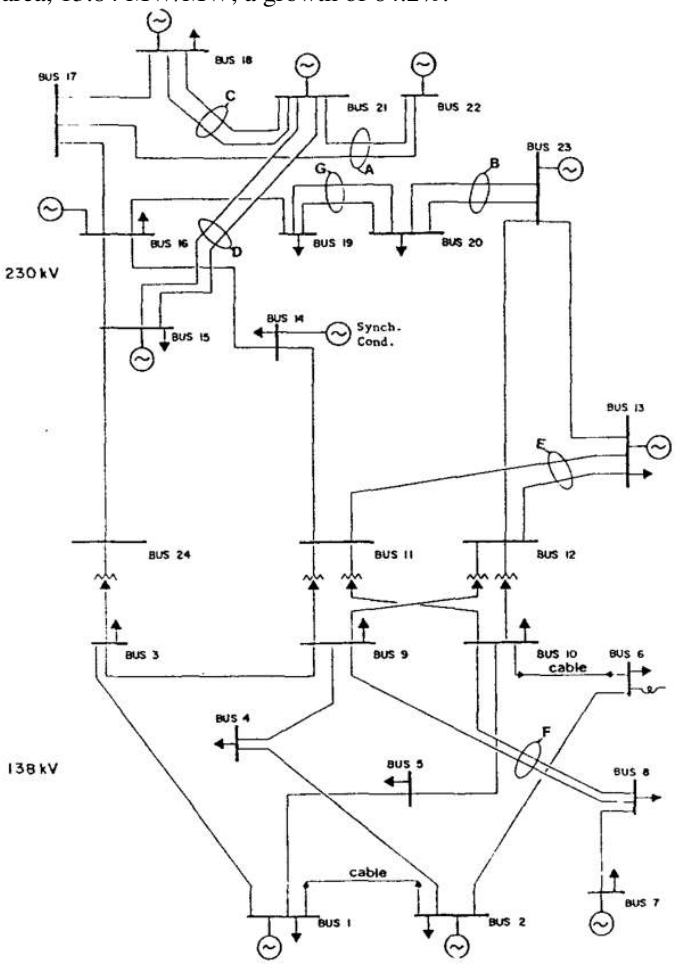

Fig. 6 Standard diagram for the RTS96 one area system, extracted from [83]

3) IEEE 118 Bus System

The representation of the IEEE 118 bus system shown in Fig. 9 is revealing: note the two very remote nodes located in the upper right portion of the figure. These two nodes, 87 and 86, are far more peripheral than the other nodes in the 138 kV system. Indeed, the authors of [96] identified bus 86 as being a very voltage-weak bus (though more remote, bus 87 is redeemed by the presence of a generator there) Separate work in [97] identified the region around bus 110 as being a potential source of voltage instability, noting that "*load increase at bus 110 results in substantial reduction of voltage at other buses surrounding it*". Such problems could be anticipated from inspection of Fig. 9, which shows the collocation of buses around 110, to the lower right, to be electrically remote from the higher voltage system, and only weakly interconnected with the broader system, with bus 100 being the sole interfacing point.

On the other hand, [96] also identified buses 20 and 33 and their neighbours as being voltage-weak, though these do not stand out in Fig. 9. Also, [92] identified a slew of potentially insecure buses which are not obvious from Fig. 9. It should be borne in mind that bus loadings and proximity to generation are also essential in appraising system voltage security, and these are not portrayed in Fig. 9, which exclusively considers impedance structure.

Comparing a standard system diagram like Fig. 7 with Fig. 8 or Fig. 9 is instructive. Most obviously, the lack of colour or thickness cues make it difficult to perceptually separate the two distinct voltage levels in Fig. 7. Furthermore, the greater extent of the 138 kV system, in electrical distance terms, is not made clear. The remote tail-fed spur connecting buses 86 and 87 is not depicted in an illuminating way, discreetly residing in the centre middle, and giving the erroneous impression that these buses possess the same level of electrical connectivity as those nodes plotted adjacent to them. Indeed, Fig. 7 seems to indicate that nodes 9 and 10 are remote buses, separated on a long radial spur, whereas Fig. 9 reveals them to be electrically close to the broader power system.

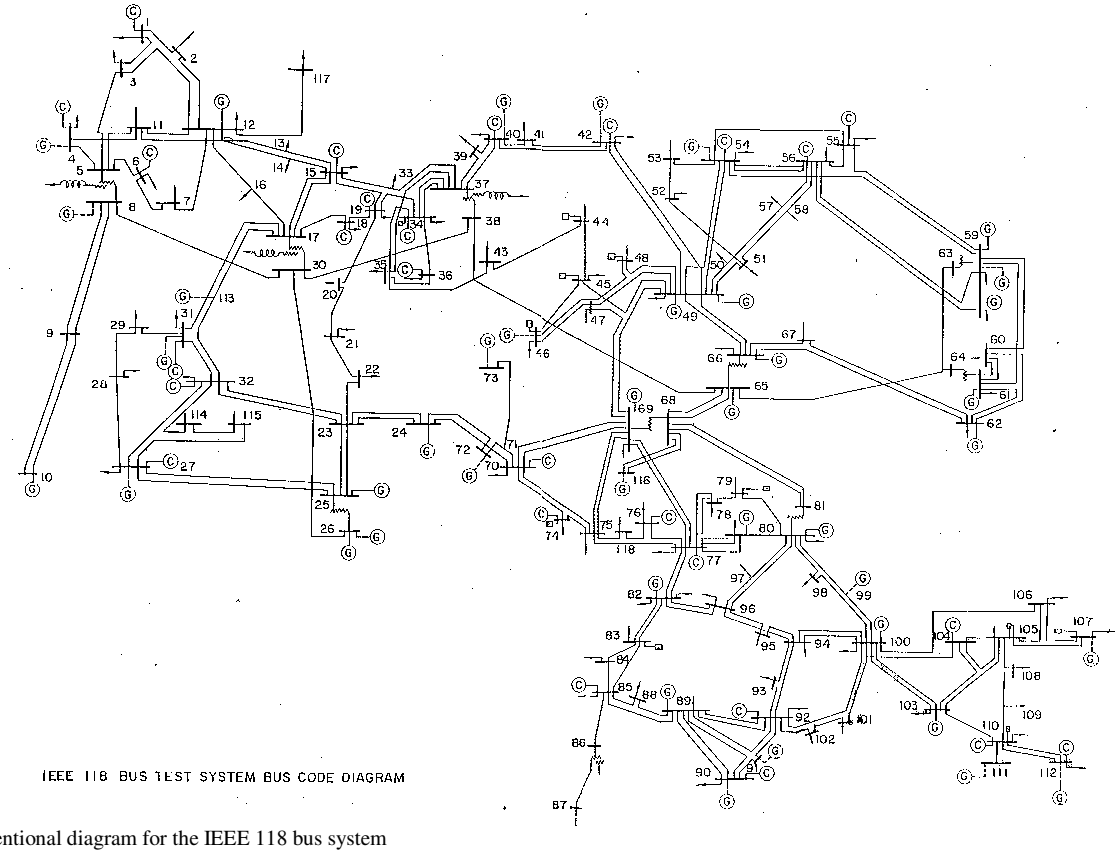

Fig. 7 A conventional diagram for the IEEE 118 bus system

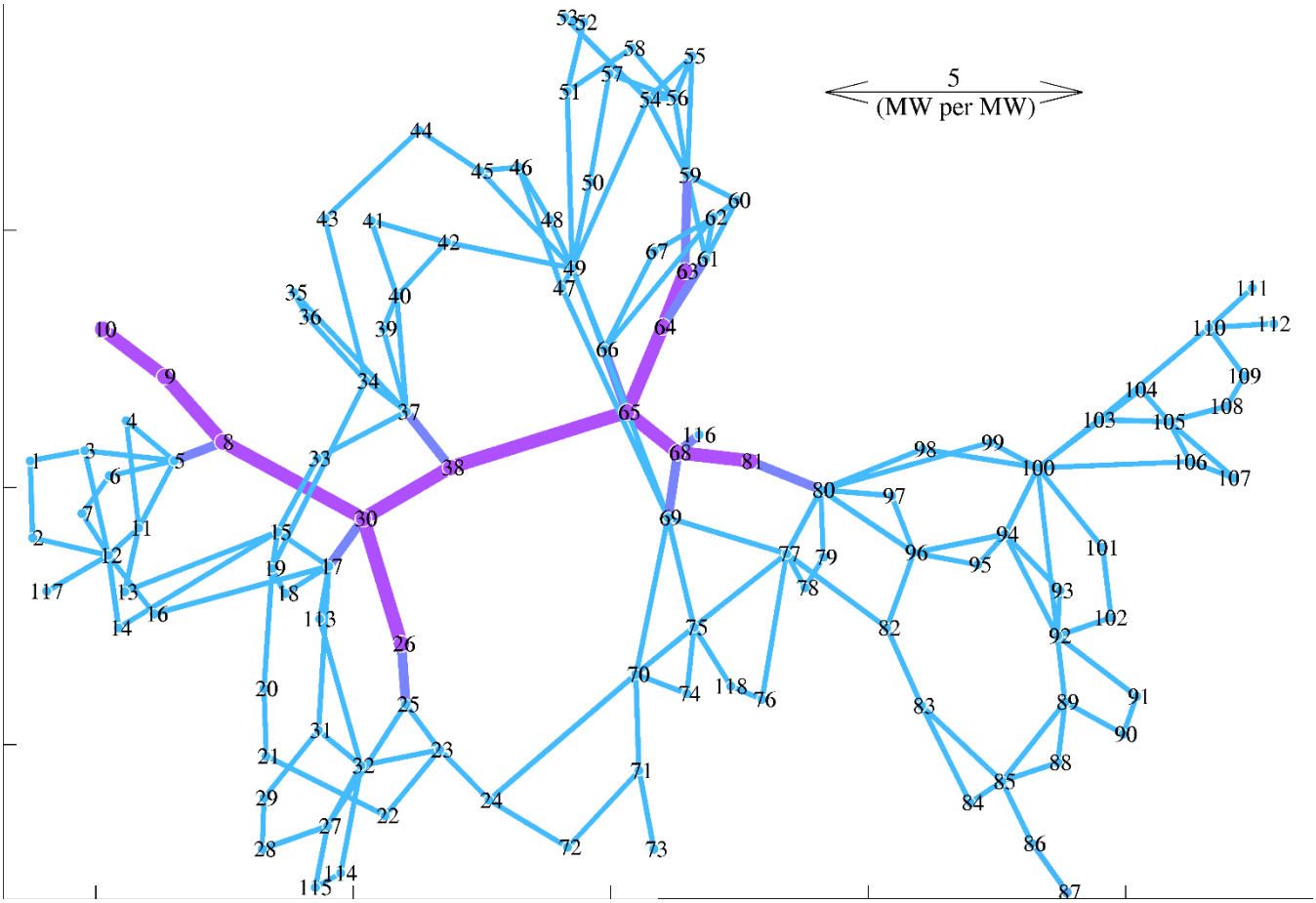

Fig. 8 The IEEE 118 bus test system, laid out to show the aggregate flow shift for each node-to-node transaction, *PT*.

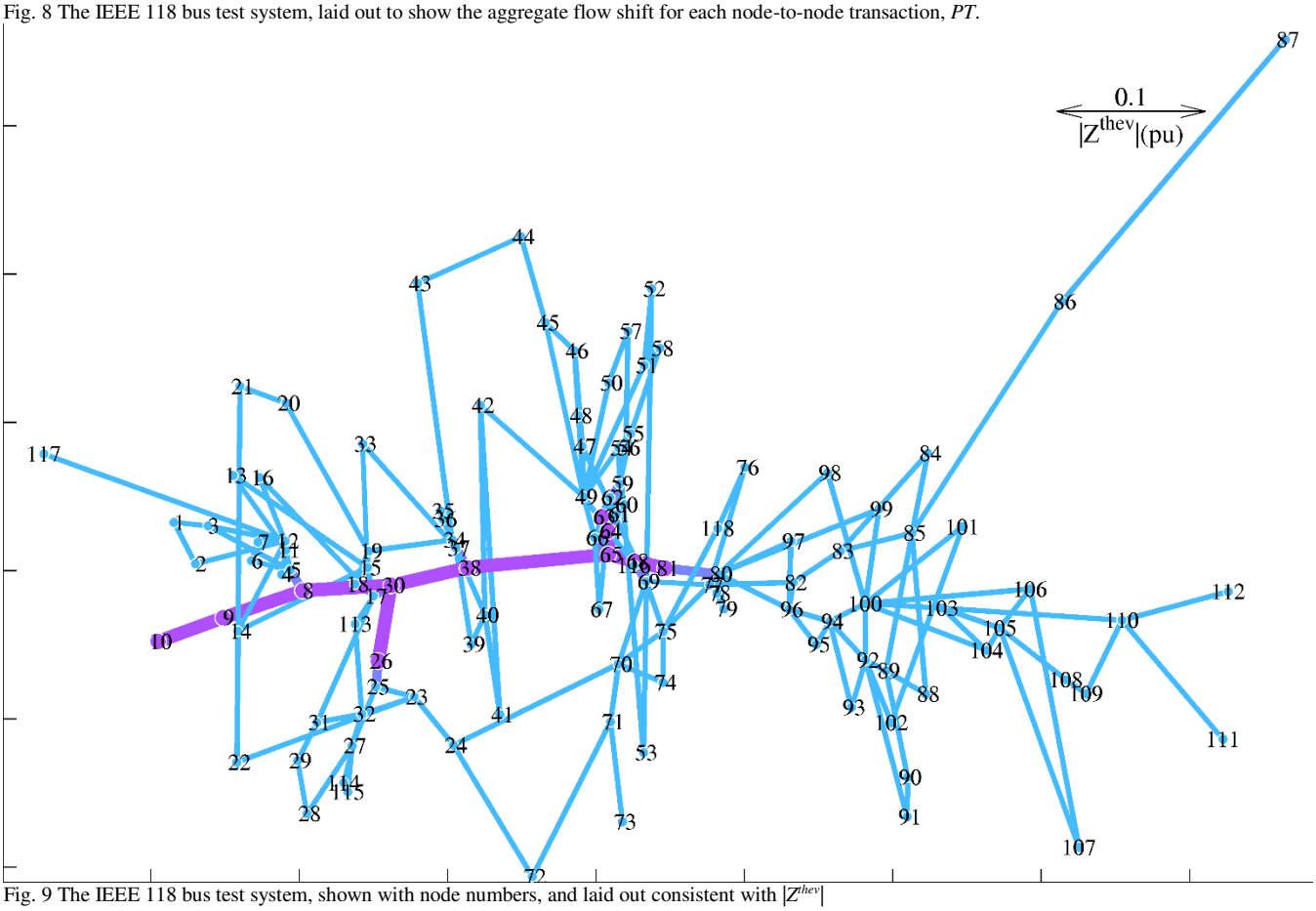

Fig. 9 The IEEE 118 bus test system, shown with node numbers, and laid out consistent with $|Z^{thev}|$

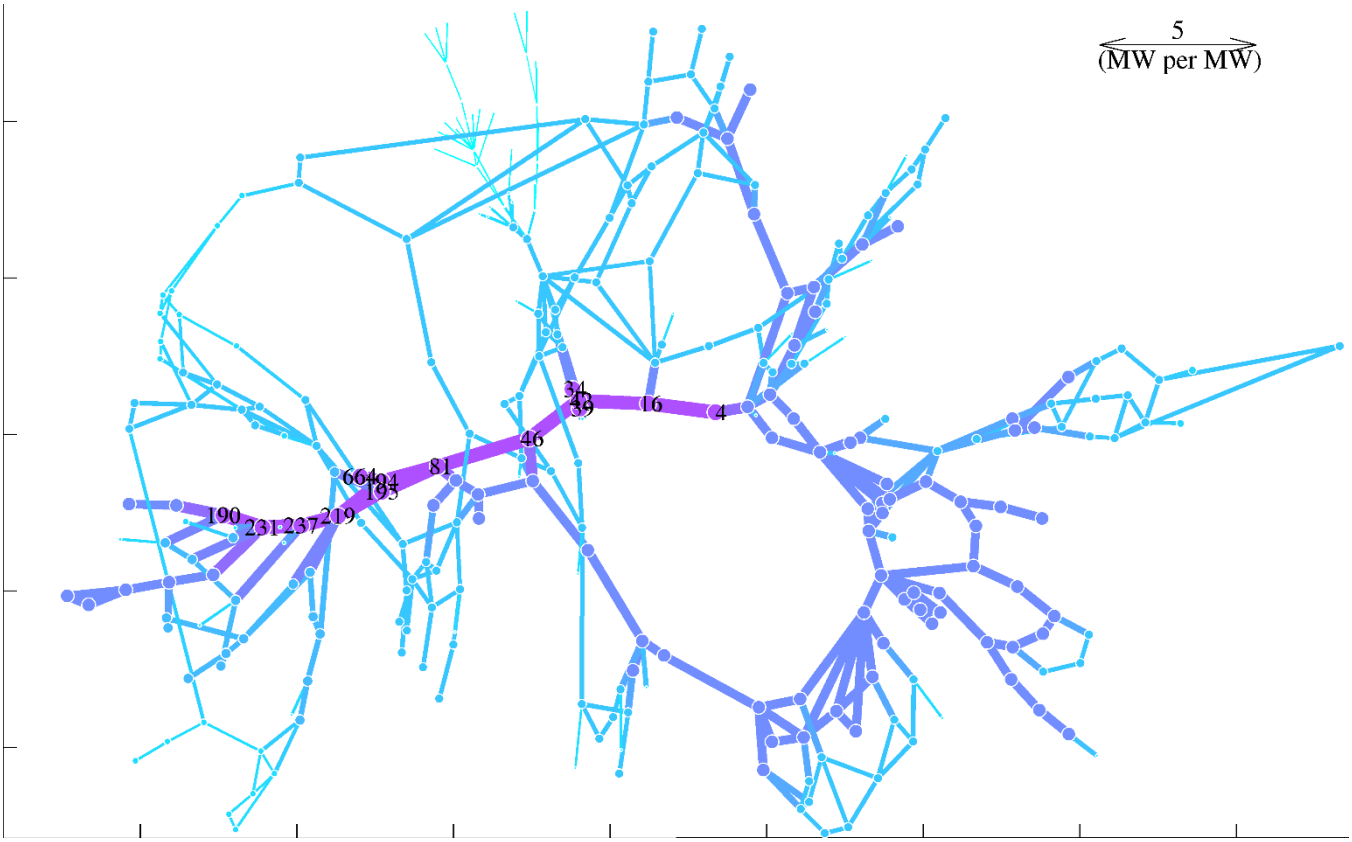

Fig. 10 The IEEE 300 bus test system laid out to show the aggregate flow shift for each node-to-node transaction

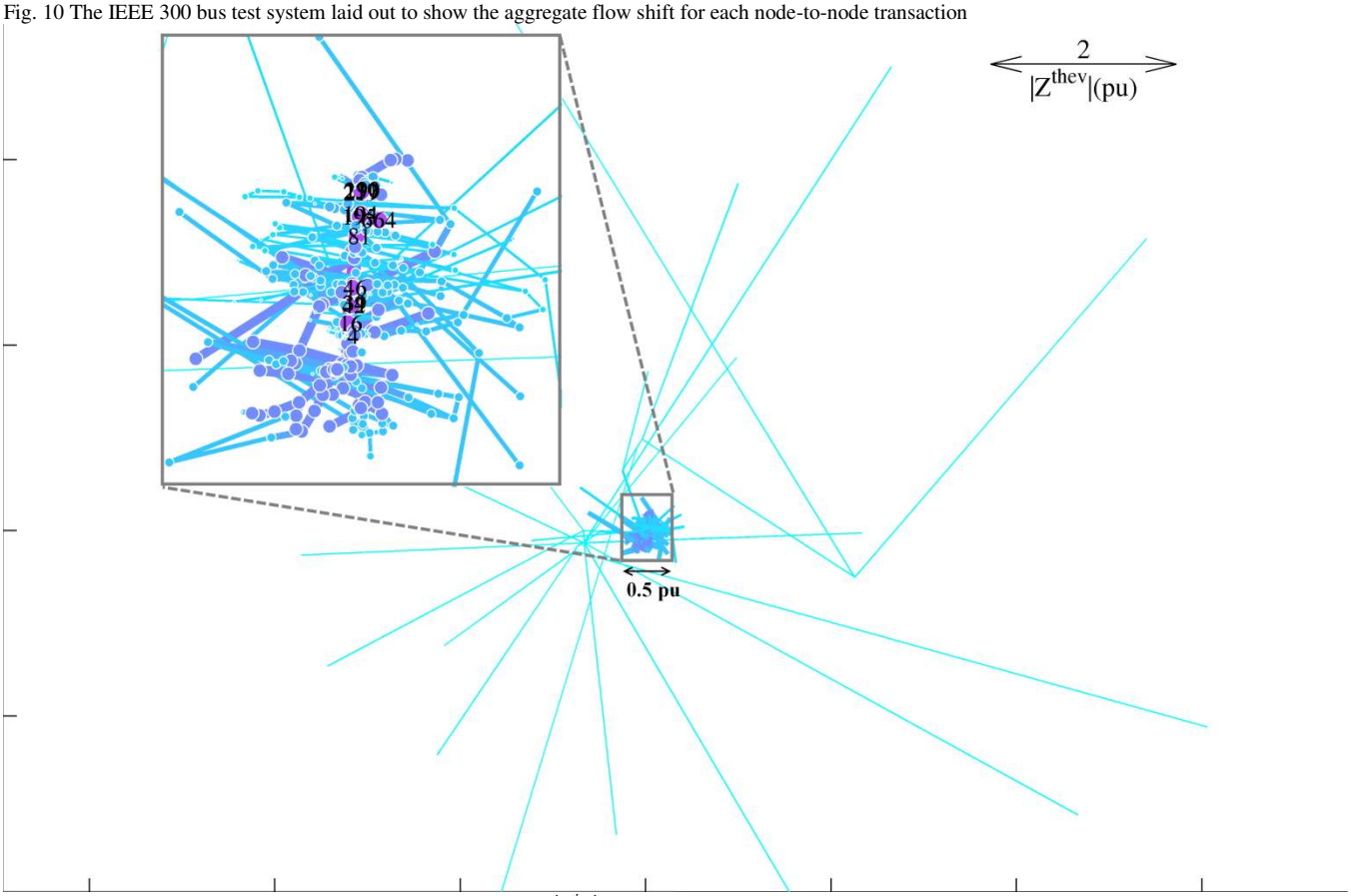

Fig. 11 The IEEE 300 bus test system, with an inset to show the $|Z^{thev}|$ impedance structure of the inner core of the system

4) IEEE 300 Bus System

The depiction of this system in Fig. 10 reveals some of its rich and complex structure. A great range of voltage levels are shown, from radial low voltage distribution networks operating between 0.6 kV and 6.6 kV (top centre-left; thin, cyan branches) to the central spine of the system, operating at 345 kV. We also observe that this system includes many leaf-nodes, that is nodes with degree $k = 1$, whereas the other systems (for instance in Fig. 2, Fig. 4 and Fig. 8) show a much greater degree of inter-node meshing. The presence of many low-voltage, and radially fed, nodes means that the $|Z^{thev}|$ structure of this network is markedly different to those of the other networks studied: Fig. 11 shows that nearly all system nodes are within a central core with diameter on ~0.3 pu, whereas around a dozen low voltage nodes sit on a periphery around this, at a remove of perhaps 5 pu. While this heterogeneity in impedance centrality does not impede the embedding into two dimensions (per Table I), it does presents challenges for presenting an uncluttered display, as even the zoomed-in inset is crowded and unclear. By contrast, the *PT* distance measure guarantees a reasonable separation between nodes, as it takes one MW/MW as a lower bound.

E. Comparison of Layout Attributes

Based on the analyses in subsections B. and C., two distance measures were selected as the underpinnings of the novel power system visualization previously discussed. The first of these measures, $|Z^{thev}|$, reveals the inherent impedance structure of the power system, and thus seems more appropriate for technical applications that are concerned with voltages, currents and power transfers. On larger systems, though, the heterogeneous nodal $|Z^{thev}|$ centrality means that resulting layouts can become cluttered and hard to interpret.

The other distance measure considered, *PT*, is more directly related to the simple topology of the system, based on power transfers under dc linearizations. It may prove insightful for market applications: what nodes can typically transact power, and how might this affect locational marginal prices? As the *PT* measure remains well bounded on larger systems, it reliably gives interpretable, aesthetically pleasing network layouts. As such layouts succinctly reveal the topological connectivity of a system, they seem a strong candidate as the default layout choice in general power system analysis applications, as their legibility surpasses that of pseudo-geographical single line diagrams.

IV. System Partitioning

The authors of [35] use sophisticated spectral techniques to portray power system nodes in two dimensions based on the system Y_{bus} matrix, an embedding which they apply to find meaningful electrical partitions of the network. The techniques presented in the present work also reveal cluster structures in power systems, and so a comparison between the two approaches can serve as a useful validation. While [35] considered both the 39 and 118 bus test systems, full results are only provided for the former, so we will restrict our comparison here to that smaller system. The partitioning shown in Fig. 12 is encouraging: the three separately-coloured areas are contiguous in our two-dimensional representation of the system's structure. As a comparison, in Fig. 13, we show a simple *K*-means clustering [98] of the two-dimensional data. Encouraging, only a small number of nodes near boundaries are assigned to a new network partition.

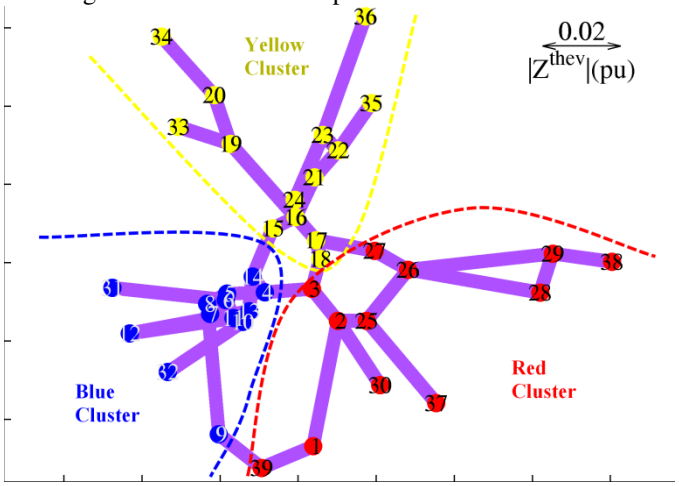

Fig. 12 The 39 bus test system, coloured to show a three-way partitioning performed using sophisticated spectral techniques in [35].

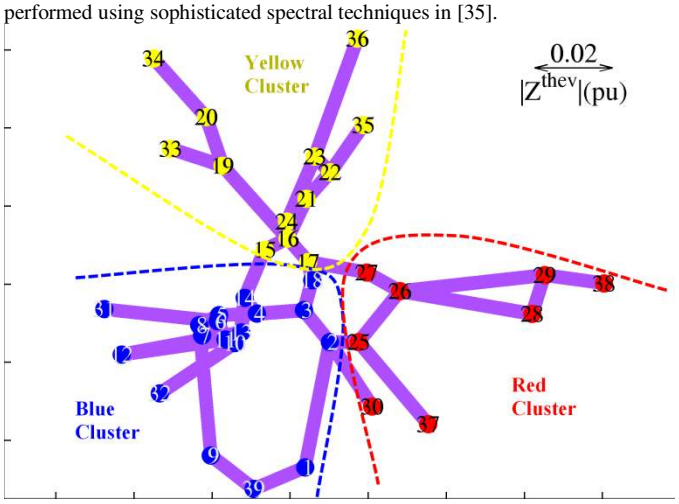

Fig. 13 The 39 bus test system, coloured to show a three-way partitioning performed using simple *K*-means partitioning of the two-dimensional data.

V. Conclusions

Certain meaningful electrical distance measures embed consistently well into two dimensions. The feasibility of this embedding, and the new perspectives it offers on the electrical structure of power systems, is the principal research contribution of the present work.

This realization suggests several new ways of portraying, analysing and reasoning about power systems.

One field that can clearly benefit from this new paradigm is voltage stability analysis. The impedance diagrams shown in this work makes the identification of voltage-weak buses quite intuitive; a load's proximity to a source of reactive power can be immediately assessed. Monitoring a system's voltage security in real time becomes more tractable with these techniques, as the new impedance structure following an outage can be intuitively grasped as the situation unfolds.

The novel observation that inter-node Thevenin impedances consistently embed well into two dimensions opens up new ways for how power system partitioning may be performed and depicted.

Power transfer distances can also be used to meaningfully position power system nodes. This may allow, for instance, the identification of system clusters that can consistently transact power amongst themselves, thus offering new ways of portraying and analysing the separation of electricity markets into distinct price zones.

The layouts based on power transfer distance enjoy greater visual separation between nodes, and so reduce clutter to give a layout that is both aesthetic and meaningful.

Finally, beyond specific technical or market applications, the novel visualizations discussed in this work are more meaningful and accessible than traditional single line diagrams; this has clear pedagogic value, as well as demystifying the power system for economists, regulators and other non-engineers in the energy ambit.

VI. References

[1] P. M. Mahadev and R. D. Christie, "Envisioning power system data: concepts and a prototype system state representation," *Power Systems, IEEE Transactions on,* vol. 8, pp. 1084-1090, 1993.

[2] E. R. Tufte, *Visual Explanations: Images and Quantities, Evidence and Narrative*: Graphics Press, 1997.

[3] E. R. Tufte, *The visual display of quantitative information*: Graphics Press, 1983.

[4] E. R. Tufte, *Envisioning Information*: Graphics Press, 2001.

[5] C. Mikkelsen, J. Johansson, and M. Cooper, "Visualization of Power System Data on Situation Overview Displays," in *Information Visualisation (IV), 2012 16th International Conference on*, 2012, pp. 188-197.

[6] T. J. Overbye and J. D. Weber, "Visualizing the electric grid," *Spectrum, IEEE,* vol. 38, pp. 52-58, 2001.

[7] T. J. Overbye, D. A. Wiegmann, A. M. Rich, and S. Yan, "Human factors aspects of power system voltage contour visualizations," *Power Systems, IEEE Transactions on,* vol. 18, pp. 76-82, 2003.

[8] J. D. Weber and T. J. Overbye, "Voltage contours for power system visualization," *Power Systems, IEEE Transactions on,* vol. 15, pp. 404-409, 2000.

[9] S. Yan and T. J. Overbye, "Visualizations for power system contingency analysis data," *Power Systems, IEEE Transactions on,* vol. 19, pp. 1859-1866, 2004.

[10] F. Milano, "Three-dimensional visualization and animation for power systems analysis," *Electric Power Systems Research,* vol. 79, pp. 1638-1647, 2009.

[11] M. J. Laufenberg, "Visualization approaches integrating real-time market data," in *Power Systems Conference and Exposition, 2004. IEEE PES*, 2004, pp. 1550-1555 vol.3.

[12] P. C. Wong, K. Schneider, P. Mackey, H. Foote, G. Chin, R. Guttromson, and J. Thomas, "A Novel Visualization Technique for Electric Power Grid Analytics," *Visualization and Computer Graphics, IEEE Transactions on,* vol. 15, pp. 410-423, 2009.

[13] Y. S. Ong, H. B. Gooi, and C. K. Chan, "Algorithms for automatic generation of one-line diagrams," *Generation, Transmission and Distribution, IEE Proceedings,* vol. 147, pp. 292-298, 2000.

[14] I. Lendak, A. Erdeljan, D. Čapko, and S. Vukmirovic, "Algorithms in electric power system one-line diagram creation," in *Systems Man and Cybernetics (SMC), 2010 IEEE International Conference on*, 2010, pp. 2867-2873.

[15] F. Belmudes, D. Ernst, and L. Wehenkel, "Pseudo-Geographical Representations of Power System Buses by Multidimensional Scaling," in *Intelligent System Applications to Power Systems, 2009. ISAP '09. 15th International Conference on*, 2009, pp. 1-6.

[16] C. McGrath, J. Blythe, and D. Krackhardt, "Seeing groups in graph layouts," *Connections,* vol. 19, pp. 22-29, 1996.

[17] F. van Ham and B. Rogowitz, "Perceptual Organization in User-Generated Graph Layouts," *Visualization and Computer Graphics, IEEE Transactions on,* vol. 14, pp. 1333-1339, 2008.

[18] T. M. J. Fruchterman and E. M. Reingold, "Graph drawing by force-directed placement," *Software: Practice and Experience,* vol. 21, pp. 1129-1164, 1991.

[19] J. Zhao, H. Zhou, B. Chen, and P. Li, "Research on the Structural Characteristics of Transmission Grid Based on Complex Network Theory," *Journal of Applied Mathematics,* vol. 2014, p. 12, 2014.

[20] S. Boccaletti, V. Latora, Y. Moreno, M. Chavez, and D. U. Hwang, "Complex networks: Structure and dynamics," *Physics Reports,* vol. 424, pp. 175-308, 2006.

[21] D. J. Watts and S. H. Strogatz, "Collective dynamics of `small-world' networks," *Nature,* vol. 393, pp. 440-442, 1998.

[22] P. Hines, S. Blumsack, E. Cotilla Sanchez, and C. Barrows, "The Topological and Electrical Structure of Power Grids," in *System Sciences (HICSS), 2010 43rd Hawaii International Conference on*, 2010, pp. 1-10.

[23] D. P. Chassin and C. Posse, "Evaluating North American electric grid reliability using the Barabási–Albert network model," *Physica A: Statistical Mechanics and its Applications,* vol. 355, pp. 667-677, 2005.

[24] R. Albert, I. Albert, and G. L. Nakarado, "Structural vulnerability of the North American power grid," *Physical review E,* vol. 69, p. 025103, 2004.

[25] V. Rosato, S. Bologna, and F. Tiriticco, "Topological properties of high-voltage electrical transmission networks," *Electric Power Systems Research,* vol. 77, pp. 99-105, 2007.

[26] W. Zhifang, A. Scaglione, and R. J. Thomas, "Generating Statistically Correct Random Topologies for Testing Smart Grid Communication and Control Networks," *Smart Grid, IEEE Transactions on,* vol. 1, pp. 28-39, 2010.

[27] E. Bompard, R. Napoli, and F. Xue, "Analysis of structural vulnerabilities in power transmission grids," *International Journal of Critical Infrastructure Protection,* vol. 2, pp. 5-12, 2009.

[28] T. A. Ernster and A. K. Srivastava, "Power system vulnerability analysis - towards validation of centrality measures," in *Transmission and Distribution Conference and Exposition (T&D), 2012 IEEE PES*, 2012, pp. 1-6.

[29] A. Dwivedi and Y. Xinghuo, "A Maximum-Flow-Based Complex Network Approach for Power System Vulnerability Analysis," *Industrial Informatics, IEEE Transactions on,* vol. 9, pp. 81-88, 2013.

[30] B. A. Carreras, D. E. Newman, I. Dobson, and A. B. Poole, "Evidence for self-organized criticality in a time series of electric power system blackouts," *Circuits and Systems I: Regular Papers, IEEE Transactions on,* vol. 51, pp. 1733-1740, 2004.

[31] A. Clauset and M. Young, "Scale invariance in global terrorism," *arXiv preprint physics/0502014,* 2005.

[32] P. Hines, E. Cotilla-Sanchez, and S. Blumsack, "Do topological models provide good information about electricity infrastructure vulnerability?," *Chaos: An Interdisciplinary Journal of Nonlinear Science,* vol. 20, pp. -, 2010.

[33] E. Cotilla-Sanchez, P. D. H. Hines, C. Barrows, and S. Blumsack, "Comparing the Topological and Electrical Structure of the North American Electric Power Infrastructure," *Systems Journal, IEEE,* vol. 6, pp. 616-626, 2012.

[34] E. Cotilla-Sanchez, P. D. H. Hines, C. Barrows, S. Blumsack, and M. Patel, "Multi-Attribute Partitioning of Power Networks Based on Electrical Distance," *Power Systems, IEEE Transactions on,* vol. 28, pp. 4979-4987, 2013.

[35] R. J. Sanchez-Garcia, M. Fennelly, S. Norris, N. Wright, G. Niblo, J. Brodzki, and J. W. Bialek, "Hierarchical Spectral Clustering of Power Grids," *Power Systems, IEEE Transactions on,* vol. 29, pp. 2229-2237, 2014.

[36] K. Wang, B.-h. Zhang, Z. Zhang, X.-g. Yin, and B. Wang, "An electrical betweenness approach for vulnerability assessment of power grids considering the capacity of generators and load," *Physica A: Statistical Mechanics and its Applications,* vol. 390, pp. 4692-4701, 2011.

[37] Y. Koç, M. Warnier, P. V. Mieghem, R. E. Kooij, and F. M. Brazier, "The impact of the topology on cascading failures in a power grid model," *Physica A: Statistical Mechanics and its Applications,* 2014.

[38] J. B. Kruskal, "Multidimensional scaling by optimizing goodness of fit to a nonmetric hypothesis," *Psychometrika,* vol. 29, pp. 1-27, 1964/03/01 1964.

[39] J. B. Kruskal, "Nonmetric multidimensional scaling: A numerical method," *Psychometrika,* vol. 29, pp. 115-129, 1964/06/01 1964.

[40] A. Buja, D. F. Swayne, M. L. Littman, N. Dean, H. Hofmann, and L. Chen, "Data Visualization With Multidimensional Scaling," *Journal of Computational and Graphical Statistics,* vol. 17, pp. 444-472, 2008/06/01 2008.

[41] J. W. Sammon, "A Nonlinear Mapping for Data Structure Analysis," *Computers, IEEE Transactions on,* vol. C-18, pp. 401-409, 1969.

[42] A. Sarveniazi, "An Actual Survey of Dimensionality Reduction," *American Journal of Computational Mathematics,* vol. 2014, 2014.

[43] P. Hines and S. Blumsack, "A Centrality Measure for Electrical Networks," in *Hawaii International Conference on System Sciences, Proceedings of the 41st Annual*, 2008, pp. 185-185.

[44] E. Bompard, E. Pons, and D. Wu, "Extended topological metrics for the analysis of power grid vulnerability," *Systems Journal, IEEE,* vol. 6, pp. 481-487, 2012.

[45] S. Arianos, E. Bompard, A. Carbone, and F. Xue, "Power grid vulnerability: A complex network approach," *Chaos: An Interdisciplinary Journal of Nonlinear Science,* vol. 19, p. 013119, 2009.

[46] P. Lagonotte, J. C. Sabonnadiere, J. Y. Leost, and J. P. Paul, "Structural analysis of the electrical system: application to secondary voltage control in France," *Power Systems, IEEE Transactions on,* vol. 4, pp. 479-486, 1989.

[47] L. Hang, A. Bose, and V. Venkatasubramanian, "A fast voltage security assessment method using adaptive bounding," *Power Systems, IEEE Transactions on,* vol. 15, pp. 1137-1141, 2000.

[48] Z. Jin, E. Nobile, A. Bose, and K. Bhattacharya, "Localized reactive power markets using the concept of voltage control areas," *Power Systems, IEEE Transactions on,* vol. 19, pp. 1555-1561, 2004.

[49] K. Visakha, D. Thukaram, and L. Jenkins, "Transmission charges of power contracts based on relative electrical distances in open access," *Electric Power Systems Research,* vol. 70, pp. 153-161, 2004.

[50] S. M. Abdelkader, "Characterization of Transmission Losses," *Power Systems, IEEE Transactions on,* vol. 26, pp. 392-400, 2011.

[51] S. M. Abdelkader, D. J. Morrow, and A. J. Conejo, "Network usage determination using a transformer analogy," *Generation, Transmission & Distribution, IET,* vol. 8, pp. 81-90, 2014.

[52] S. M. Abdelkader, "A new method for transmission loss allocation considering the circulating currents between generators," in *Power System Conference, 2008. MEPCON 2008. 12th International Middle-East*, 2008, pp. 282-286.

[53] U. Brandes, P. Kenis, and J. Raab, "Explanation Through Network Visualization," *Methodology: European Journal of Research Methods for the Behavioral and Social Sciences,* vol. 2, pp. 16-23, 2006.

[54] R. Merris, "Laplacian matrices of graphs: a survey," *Linear Algebra and its Applications,* vol. 197–198, pp. 143-176, 1994.

[55] D. J. Klein and M. Randić, "Resistance distance," *Journal of Mathematical Chemistry,* vol. 12, pp. 81-95, 1993/12/01 1993.

[56] A. K. Saxena and D. Anand Rao, "A new approach to bus impedance matrix building," *Computers & Electrical Engineering,* vol. 29, pp. 55-65, 2003.

[57] H. R. E. Bouchekara. (2011, Power System Analysis: The Impedance Model and Network Calculations (course notes). Available: https://uqu.edu.sa/hnbouchekara/ar/200404

[58] A. Tizghadam and A. Leon-Garcia, "Betweenness centrality and resistance distance in communication networks," *Network, IEEE,* vol. 24, pp. 10-16, 2010.

[59] P. W. Fowler, "Resistance distances in fullerene graphs," *Croatica chemica acta,* vol. 75, pp. 401-408, 2002.

[60] B. H. McRae, "Isolation By Resistance," *Evolution,* vol. 60, pp. 1551-1561, 2006.

[61] F. Edström, "On eigenvalues to the Y-bus matrix," *International Journal of Electrical Power & Energy Systems,* vol. 56, pp. 147-150, 2014.

[62] K. Purchala, L. Meeus, D. Van Dommelen, and R. Belmans, "Usefulness of DC power flow for active power flow analysis," in *Power Engineering Society General Meeting, 2005. IEEE*, 2005, pp. 454-459 Vol. 1.

[63] B. Stott, J. Jardim, and O. Alsac, "DC Power Flow Revisited," *Power Systems, IEEE Transactions on,* vol. 24, pp. 1290-1300, 2009.

[64] I. Dobson, M. Parashar, and C. Carter, "Combining Phasor Measurements to Monitor Cutset Angles," in *System Sciences (HICSS), 2010 43rd Hawaii International Conference on*, 2010, pp. 1-9.

[65] V. M. Venkatasubramanian, Y. Xunning, L. Guoping, M. Sherwood, and Z. Qiang, "Wide-Area monitoring and control algorithms for large power systems using synchrophasors," in *Power Systems Conference and Exposition, 2009. PSCE '09. IEEE/PES*, 2009, pp. 1-5.

[66] S. Pérez-Londoño, L. F. Rodríguez, and G. Olivar, "A Simplified Voltage Stability Index (SVSI)," *International Journal of Electrical Power & Energy Systems,* vol. 63, pp. 806-813, 2014.

[67] J. G. Vlachogiannis, "Simplified reactive power management strategy for complex power grids under stochastic operation and incomplete information," *Energy Conversion and Management,* vol. 50, pp. 3193-3201, 2009.

[68] W. Ellens, F. Spieksma, P. Van Mieghem, A. Jamakovic, and R. Kooij, "Effective graph resistance," *Linear Algebra and its Applications,* vol. 435, pp. 2491-2506, 2011.

[69] L. Lovász, "Random walks on graphs: A survey," *Combinatorics, Paul erdos is eighty,* vol. 2, pp. 1-46, 1993.

[70] I. Gutman and B. Mohar, "The Quasi-Wiener and the Kirchhoff Indices Coincide," *Journal of Chemical Information and Computer Sciences,* vol. 36, pp. 982-985, 1996/01/01 1996.

[71] W. Xiao and I. Gutman, "Resistance distance and Laplacian spectrum," *Theoretical Chemistry Accounts,* vol. 110, pp. 284-289, 2003/11/01 2003.

[72] R. B. Bapat, I. Gutman, and W. Xiao, "A simple method for computing resistance distance," *Zeitschrift fur Naturforschung A,* vol. 58, pp. 494-498, 2003.

[73] T. H. Sikiru, A. A. Jimoh, Y. Hamam, J. T. Agee, and R. Ceschi, "Classification of networks based on inherent structural characteristics," in *Transmission and Distribution: Latin America Conference and Exposition (T&D-LA), 2012 Sixth IEEE/PES*, 2012, pp. 1-6.

[74] F. Edström and L. Söder, "On spectral graph theory in power system restoration," in *Innovative Smart Grid Technologies (ISGT Europe), 2011 2nd IEEE PES International Conference and Exhibition on*, 2011, pp. 1-8.

[75] B. C. Lesieutre, S. Roy, V. Donde, and A. Pinar, "Power System Extreme Event Screening using Graph Partitioning," in *Power Symposium, 2006. NAPS 2006. 38th North American*, 2006, pp. 503-510.

[76] T. H. Sikiru, A. A. Jimoh, and J. T. Agee, "Inherent structural characteristic indices of power system networks," *International Journal of Electrical Power & Energy Systems,* vol. 47, pp. 218-224, 2013.

[77] R. D. Christie, B. F. Wollenberg, and I. Wangensteen, "Transmission management in the deregulated environment," *Proceedings of the IEEE,* vol. 88, pp. 170-195, 2000.

[78] U. Brandes and D. Fleischer, "Centrality Measures Based on Current Flow," in *STACS 2005*. vol. 3404, V. Diekert and B. Durand, Eds., ed: Springer Berlin Heidelberg, 2005, pp. 533-544.

[79] A. J. Conejo, E. Castillo, R. Minguez, and F. Milano, "Locational marginal price sensitivities," *Power Systems, IEEE Transactions on,* vol. 20, pp. 2026-2033, 2005.

[80] T. Greville, "Some Applications of the Pseudoinverse of a Matrix," *SIAM Review,* vol. 2, pp. 15-22, 1960.

[81] E. W. Dijkstra, "A note on two problems in connexion with graphs," *Numerische mathematik,* vol. 1, pp. 269-271, 1959.

[82] W. H. Kersting, "Radial distribution test feeders," *Power Systems, IEEE Transactions on,* vol. 6, pp. 975-985, 1991.

[83] C. Grigg, P. Wong, P. Albrecht, R. Allan, M. Bhavaraju, R. Billinton, Q. Chen, C. Fong, S. Haddad, S. Kuruganty, W. Li, R. Mukerji, D. Patton, N. Rau, D. Reppen, A. Schneider, M. Shahidehpour, and C. Singh, "The IEEE Reliability Test System-1996. A report prepared by the Reliability Test System Task Force of the Application of Probability Methods Subcommittee," *Power Systems, IEEE Transactions on,* vol. 14, pp. 1010-1020, 1999.

[84] O. Alsac and B. Stott, "Optimal Load Flow with Steady-State Security," *Power Apparatus and Systems, IEEE Transactions on,* vol. PAS-93, pp. 745-751, 1974.
[85] T. Athay, R. Podmore, and S. Virmani, "A Practical Method for the Direct Analysis of Transient Stability," *Power Apparatus and Systems, IEEE Transactions on,* vol. PAS-98, pp. 573-584, 1979.
[86] R. Christie. (1993). *"Power System Test Case Archive"*. Available: http://www.ee.washington.edu/research/pstca/
[87] The MathWorks Inc. MATLAB and Statistics Toolbox Release 2013a.
[88] R. D. Zimmerman, C. E. Murillo-Sánchez, and R. J. Thomas, "MATPOWER: Steady-State Operations, Planning, and Analysis Tools for Power Systems Research and Education," *Power Systems, IEEE Transactions on,* vol. 26, pp. 12-19, 2011.
[89] I. Borg and P. J. F. Groenen, "MDS Models and Measures of Fit," in *Modern Multidimensional Scaling*, ed: Springer New York, 2005, pp. 37-61.
[90] K. Sturrock and J. Rocha, "A Multidimensional Scaling Stress Evaluation Table," *Field Methods,* vol. 12, pp. 49-60, February 1, 2000 2000.
[91] R. MacCallum, "Evaluating Goodness of Fit in Nonmetric Multidimensional Scaling by ALSCAL," *Applied Psychological Measurement,* vol. 5, pp. 377-382, 1981.
[92] P. Acharjee, "Identification of maximum loadability limit and weak buses using security constraint genetic algorithm," *International Journal of Electrical Power & Energy Systems,* vol. 36, pp. 40-50, 2012.
[93] P. Cuffe, E. Lannoye, A. Keane, and A. Tuohy, "Unit Commitment Considering Regional Synchronous Reactive Power Requirements: Costs and Effects," presented at the 11th Wind Integration Workshop, Lisbon, Portugal, 2012.
[94] P. M. Subcommittee, "IEEE Reliability Test System," *Power Apparatus and Systems, IEEE Transactions on,* vol. PAS-98, pp. 2047-2054, 1979.
[95] R. N. Allan, R. Billinton, and N. M. K. Abdel-Gawad, "The IEEE Reliability Test System - Extensions to and Evaluation of the Generating System," *Power Systems, IEEE Transactions on,* vol. 1, pp. 1-7, 1986.
[96] P. Rao, M. L. Crow, and Y. Zhiping, "STATCOM control for power system voltage control applications," *Power Delivery, IEEE Transactions on,* vol. 15, pp. 1311-1317, 2000.
[97] V. Balamourougan, T. S. Sidhu, and M. S. Sachdev, "Technique for online prediction of voltage collapse," *Generation, Transmission and Distribution, IEE Proceedings-,* vol. 151, pp. 453-460, 2004.
[98] J. MacQueen, "Some methods for classification and analysis of multivariate observations," in *Proceedings of the Fifth Berkeley Symposium on Mathematical Statistics and Probability, Volume 1: Statistics*, Berkeley, Calif., 1967, pp. 281-297.

Paul Cuffe (S'07-M'14) received B.E. and Ph.D. degrees in Electrical Engineering from University College Dublin in 2009 and 2013, respectively. He is currently a senior researcher within the Electricity Research Centre, University College Dublin (UCD), Ireland. His research interests are in reactive power management, distribution generation and power system visualization techniques. (paul.cuffe@ucd.ie)

Andrew Keane (S'04–M'07-SM'14) received the B.E. and Ph.D. degrees in electrical engineering from University College Dublin, Ireland, in 2003 and 2007, respectively. He is currently a Senior Lecturer with the School of Electrical, Electronic, and Communications Engineering, University College Dublin. He has previously worked with ESB Networks, the Irish Distribution System Operator. His research interests include power systems planning and operation, distributed energy resources, and distribution networks.